TRENDS IN SCIENCES 2026; 23(4): 11659
https://doi.org/10.48048/tis.2026.11659 RESEARCH ARTICLE

Synthesis of *N,N*-Dimethylcyclohexylamine-Hyptolide and Activity Assessment Against Breast Cancer Stem Cells (BCSCs) Using *In Vitro* and *In Silico* Approaches

Meiny Suzery[1,*], Lulut Tutik Margi Rahayu[2], Parsaoran Siahaan[1] and Bambang Cahyono[1]

[1]*Chemistry Department, Faculty of Sciences and Mathematics, Diponegoro University, Semarang, Indonesia*
[2]*Postgraduate Chemistry Program, Faculty of Sciences and Mathematics, Diponegoro University, Semarang, Indonesia*

([*]Corresponding author's e-mail: meiny.suzery@live.undip.ac.id)

Received: 22 August 2025, Revised: 15 September 2025, Accepted: 25 September 2025, Published: 30 December 2025

Abstract

The overexpression of histone deacetylase (HDAC) proteins in breast cancer stem cells (BCSCs) significantly contributes to tumor progression, chemotherapy resistance, and impaired apoptotic signaling through the silencing of tumor suppressor genes. Targeting HDAC with small-molecule inhibitors is therefore considered a promising therapeutic strategy. In this study, a novel hyptolide-based compound, *N,N*-dimethylcyclohexylamine-hyptolide (compound **3**), was successfully synthesized via a Diels-Alder reaction. The compound was structurally characterized using FTIR, ^{1}H-NMR, ^{13}C-NMR and TLC-MS, confirming the formation of a cyclohexene ring bearing a tertiary amine group. The product exhibited a melting point of 83 - 84 °C and a molecular weight of 595 g/mol. *In vitro* cytotoxicity assays on BCSCs revealed an IC_{50} value of 47.42 µg/mL, classifying it as moderately active and indicating its potential as a therapeutic candidate for BCSCs. Moreover, flow cytometry analysis demonstrated that the compound induced cell cycle arrest at both the S phase (DNA synthesis) and the G2/M phase (cell division). Complementary *in silico* molecular docking simulations showed stable binding interactions between the compound and key active-site residues of HDAC, supporting its potential as an HDAC inhibitor. These findings suggest that *N,N*-dimethylcyclohexylamine-hyptolide may serve as a promising lead for the development of HDAC-targeted therapies, particularly in the treatment of aggressive and drug-resistant breast cancers.

Keywords: Hyptolide, Diels-Alder synthesis, Breast cancer stem cells, Cell cycle arrest, Molecular docking

Introduction

Breast cancer remains one of the leading causes of cancer-related mortality among women worldwide, with its global burden continuing to rise annually. According to the World Health Organization (2022), approximately 2.3 million women were diagnosed with breast cancer, resulting in 670.000 deaths globally. Among the various molecular subtypes of breast cancer, triple-negative breast cancer (TNBC) poses the greatest clinical challenge due to its highly aggressive nature, absence of targeted hormonal receptors, and poor response to conventional chemotherapy. A growing body of evidence highlighted the pivotal role of Breast Cancer Stem Cells (BCSCs) in the pathogenesis, progression, and recurrence of TNBC. These cells possess self-renewal capabilities and are known to contribute to drug resistance, tumor relapse, and metastasis [1]. BCSCs frequently overexpress ATP-binding cassette (ABC) transporters, which actively efflux chemotherapeutic agents out of the cells, reducing their cytotoxic efficacy. Moreover, BCSCs tend to evade apoptosis and persist even after aggressive treatment, emphasizing the urgent need for novel therapeutic strategies specifically designed to eliminate this subpopulation [2].

One promising approach involves targeting epigenetic regulators, such as histone deacetylases (HDACs). HDACs are enzymes that remove acetyl groups from histone proteins, leading to chromatin

condensation and transcriptional repression [3]. Overexpression of HDACs in cancer cells has been linked to the silencing of tumor suppressor genes, deregulated cell cycle progression, and reduced apoptosis [4]. Consequently, HDACs has emerged as a validated therapeutic targets, and several HDAC inhibitors have entered clinical trials. However, the clinical efficacy of existing synthetic inhibitors remains limited due to toxicity and non-selectivity. This has driven interest in the exploration of natural compounds and their derivatives with HDAC-inhibitory properties. Recent therapeutic strategies increasingly focus on targeting BCSCs using natural products and synthetic derivatives, which demonstrate selective cytotoxicity and the ability to suppress stemness-associated pathways [5-7]. Studies such as those by Jenie *et al.* [5] highlight promising bioactive compounds capable of overcoming chemo-resistance through induction of apoptosis and inhibition of cell cycle progression in BCSCs. Despite these advances, there remains a pressing need for compounds with enhanced specificity, improved bioavailability, and greater metabolic stability to effectively disrupt BCSC functions without harming normal stem cell populations.

Hyptolide **(1)**, a naturally occurring compound isolated from *Hyptis pectinata* (L.) Poit., has attracted attention due to its broad-spectrum bioactivity, including anticancer, antiplasmodial, and antibacterial effects [7-9]. Previous studies have shown that Hyptolide **(1)** and its derivatives exhibit significant cytotoxic activity against various cancer cell lines. For instance, Barbosa *et al.* [10] reported strong inhibitory effects of H. pectinata extracts on colon (HCT-8) and glioblastoma (SF-295) cancer cells [10]. Derivatives such as epoxyhyptolide, pectinolide J, and pectinolide E have demonstrated cytotoxicity against MDA-MB-231 breast cancer cells, with IC_{50} values of 15.2 ± 1.1 and 28.5 ± 1.8 µg/mL, respectively [11]. In addition, Suzery *et al.* [7] reported hyptolide's IC_{50} of 76.76 µg/mL against MCF-7 and 5.6 ± 0.4 µg/mL against MDA-MB-231 breast cancer cells [7]. Given the *α,β*-unsaturated *δ*-lactone structure of Hyptolide **(1)**, further chemical modifications may enhance its bioactivity and target specificity. One approach involves functionalization via a Diels-Alder reaction with trans-3-(tert-butyldimethylsilyloxy)-*N,N*-dimethyl-1,3-butadiene-1-amine **(2)**, introducing electron-donating and tertiary amine groups that potentially improve molecular interaction with HDAC's active sites [12].

A major limitation in current research is the insufficient exploration of chemical modifications that can improve the pharmacological properties of natural products to better target BCSC regulatory proteins. In this context, the incorporation of a tertiary amine moiety, as in *N,N*-dimethylcyclohexylamine-hyptolide **(3)**, offers a promising approach. This structural modification enhances compound polarity and potential interactions with proteins such as histone deacetylases (HDACs), supported by Insilico docking simulations as a comprehensive method. By improving cellular uptake and metabolic stability, *N,N*-dimethylcyclohexylamine-hyptolide **(3)** is hypothesized to more effectively induce cell cycle arrest and apoptosis in BCSCs than its parent compound, Hyptolide **(1)**. Thus, this study aims to fill the existing research gap by evaluating the anticancer efficacy of a tertiary amine-modified natural product derivative, potentially advancing the development of novel therapeutics targeting breast cancer stem cells.

Materials and methods

Materials

The materials used in the synthesis stage included Hyptolide **(1)** obtained through isolation, Trans-3-(tert-butyldimethylsilyloxy)-*N,N*-dimethyl-1,3-butadiene-1-amine **(2)**, dichloromethane, ethyl acetate, diethyl ether, methanol, and chloroform, all of which were purchased from Sigma-Aldrich (St. Louis, MO, USA) and Merck (Darmstadt, Germany). The solvents employed were of analytical grade (Merck, Darmstadt, Germany). Thin layer chromatography (TLC) was conducted using silica gel plates (Kieselgel 60 F254, 0.20 mm, Merck, Darmstadt, Germany), with the synthesized compounds detected under UV light at wavelengths of 245 and 366 nm. Melting points were determined using a Fischer John apparatus. Infrared spectra were recorded using a FTIR Spectrum 2 FT-IR Spectrometer (PerkinElmer, USA). Thin Layer Chromatography-Mass Spectrometry (TLC-MS) analysis was performed with a Plate Express® Automated TLC plate reader (Advion Interchim Scientific, New York, USA). Proton nuclear magnetic resonance (^{1}H-NMR) spectra were acquired at 400 MHz in $CDCl_3$ using a Jeol JNM-ECA spectrometer (Jeol, Tokyo, Japan).

Methods

General procedure for the synthesis of *N,N*-dimethylcyclohexylamine-hyptolide (3)

The synthesis of *N,N*-dimethylcyclohexylamine-hyptolide **(3)** was performed by adapting the procedure reported by Kozmin *et al.* [11]. Trans-3-(tert-butyldimethylsilyloxy)-*N,N*-dimethyl-1,3-butadiene-1-amine **(2)** (0.67 mmol) was dissolved in 10 mL of diethyl ether in a 3-neck round-bottom flask. Hyptolide **(1)** (1.35 mmol) was added in one portion to the solution, and the reaction mixture was stirred for 32 h at 20 °C, yielding a pale-yellow solution. The reaction was monitored by thin-layer chromatography (TLC). Upon completion, the reaction mixture was concentrated under reduced pressure using a rotary evaporator. The crude solid was dissolved in chloroform and purified by preparative thin layer chromatography (prep-TLC). The purified product was filtered, dried in a desiccator vacuum, and its purity was confirmed through single- and 2-dimensional TLC as well as melting point analysis. The pure synthesized compound was then characterized using FTIR spectroscopy, TLC-MS, and NMR The general reaction conditions for the synthesis of *N,N*-dimethylcyclohexylamine-hyptolide (3) are summarized in **Table 1** for clarity and easy comparison.

Tabel 1 Reaction conditions for the synthesis of *N,N*-dimethylcyclohexylamine-hyptolide (3) via diels-alder reaction.

Parameter	Details
Reaction type	Diels-Alder reaction
Reactants	Hyptolide **(1)** and **t**rans-3-(tert-butyldimethylsilyloxy)-*N,N*-dimethyl-1,3-butadiene-1-amine **(2)**
Molar ratio	2:1 (Hyptolide: Diene)
Solvent	Diethyl ether
Solvent volume	10 mL
Temperature	20 ℃
Reaction time	32 h
Monitoring method	Thin-layer chromatography (TLC)
Puri	Preparative thin-layer chromatography (prep-TLC)
Characterization Techniques	FTIR, ^{1}H-NMR, ^{13}C-NMR, TLC-MS, melting point analysis

Determination of the functional groups using FTIR

A PerkinElmer® Frontier™ FTIR spectrophotometer (Waltham, MA, USA) was used to identify the functional groups present in the *N,N*-dimethylcyclohexylamine-hyptolide **(3)** compound by conducting 3 scans over a spectral range of 5,500 - 435 cm^{-1} with a resolution of 4.0 cm^{-1}.

Determination of purity compound using TLC/MS

Thin-layer Chromatography-Mass Spectrometry (TLC-MS) was performed using a Plate Express® Automated TLC plate reader (Advion Interchim Scientific, New York, USA) to determine the mass spectrum of the synthesized *N,N*-dimethylcyclohexylamine-hyptolide **(3)** compound directly from spots on the TLC plates. The mass spectrometer employed the Atmospheric Pressure Chemical Ionization (APCI) method in positive ion mode, detecting ions such as $[M + H]^+$ and $[M + Na]^+$.

Determination of the structure of compound using ^{1}H-NMR and ^{13}C-NMR

The proton and carbon NMR spectra were recorded on a Jeol Resonance at 400 MHz, with $CDCl_3$ used as both the solvent and reference standard. The ^{1}H-NMR spectrum enabled identification of the number, type and arrangement of hydrogen atoms in *N,N*-dimethylcyclohexylamine-hyptolide **(3)**. The ^{13}C-NMR spectrum allowed for the determination of the number and chemical environments of the carbon atoms present in the compound [13].

Breast cancer stem cell (BCSCs) isolation and validation

MDAMB-231 human breast cancer cells (#HTB26, ATCC, Manassas, VA, USA) were cultured in high glucose Dulbecco's Modified Eagle's Medium (DMEM) (Gibco, USA) supplemented with 10% fetal bovine serum (Gibco, USA), 12.5 µg/mL amphotericin B (Gibco, USA), 150 µg/mL streptomycin, and 150 IU/mL penicillin (Gibco, USA). The cells were maintained at 37 °C in a humidified atmosphere containing 5 % CO_2 [13]. The presence of breast cancer stem cells (BCSCs) within the MDAMB-231 cell population was subsequently analyzed by flow cytometry using CD44 and CD24 antibodies conjugated to magnetic microbeads (Miltenyi Biotec Inc., CA). BCSCs were identified based on the $CD44^+/CD24^-$ cell population. Isolation of this BCSC subpopulation, characterized by $CD44^+$ and $CD24^-$ surface expression, was performed using the magnetic activated cell sorting (MACS) system with anti-CD44 and anti-CD24-biotin antibodies combined with anti-biotin microbeads (Miltenyi Biotec Inc., CA) [14]. Positive and negative selections were carried out sequentially using MS and LD columns, respectively (Miltenyi Biotec Inc., CA). The $CD44^+/CD24^-$ phenotype was confirmed by flow cytometry (BD Biosciences, Franklin Lakes, New Jersey) using anti-CD44-FITC and anti-CD24-PE monoclonal antibodies (BD Biosciences, Franklin Lakes, New Jersey) [5,15].

Cytotoxicity assays against *Breast Cancer Stem Cells* (BCSCs)

The cytotoxicity assay was performed using the MTT method on Breast Cancer Stem Cells (BCSCs) [16]. BCSCs were seeded at a density of 2×10^4 cells/mL in 96-well plates and incubated for 24 h. Subsequently, *N,N*-dimethylcyclohexylamine-hyptolide **(3)** was added at varying concentrations of 2.5, 5, 10, 25, and 50 µg/mL. Untreated cells served as the negative control (MDEM medium containing 0.01% DMSO). After another 24-hour incubation, the culture medium was removed and replaced with 0.5 mg/mL MTT reagent (Sigma-Aldrich), followed by incubation for 4 h at 37 °C in a 5% CO_2 incubator. The formation of formazan crystals, resulting from the mitochondrial conversion of MTT, was stopped by adding SDS (sodium dodecyl sulfate) dissolved in 0.01 N HCl, and the mixture was incubated for 24 h at room temperature. DMSO was then added to dissolve the formed formazan crystals. Absorbance was measured at 595 nm using an ELISA reader (Biorad iMark™ Microplate Reader) [17]. The IC_{50} value, defined as the concentration that inhibits 50% of cell growth, was calculated using linear regression with the equation $y = ax + c$, where y represents the percentage of cell viability, and x is the concentration corresponding to $y = 50$. The IC_{50} of *N,N*-dimethylcyclohexylamine-hyptolide **(3)** was compared to that of Hyptolide **(1)** for the same cell inhibition assay [14].

Cell cycle analysis

Cell cycle distribution was analyzed using flow cytometry (DB Accuri C6 Plus, BD Biosciences, USA). Breast Cancer Stem Cells (MDAMB-231) were cultured in 6-well plates and treated with *N,N*-dimethylcyclohexylamine-hyptolide **(3)** at concentrations of 55 and 110 µg/mL, with doxorubicin serving as a positive control, followed by incubation for 24 h. The cells were then harvested using EDTA-free trypsin and washed twice with pre-cooled phosphate-buffered saline (PBS) and methanol, before being incubated at 4 °C for 15 min. Each tube was then treated with BD Cycletest reagent (BD Biosciences, USA), consisting of 100 µL propidium iodide (PI) (50 µg/mL) and 10 µL RNase A (50 µg/mL), and incubated for 30 min at room temperature, according to the manufacturer's instructions [5].

Molecular docking and molecular dynamics simulation

In this study, a molecular docking analysis was conducted to examine the binding interactions between the ligand *N,N*-dimethylcyclohexylamine-hyptolide **(3)** and the HDAC protein receptor, with hydroxamic acid serving as the positive control. This computational approach was employed to support the findings obtained from the *in vitro* experiments. Molecular docking was performed using AutoDockTools 1.5.7, while molecular dynamics simulations were carried out using Yet Another Scientific Artificial Reality Application (YASARA). The HDAC receptor sequence (PDB ID: 3C0Y) was retrieved from the RCSB Protein Data Bank (http://www.rcsb.org/pdb/). The structures of *N,N*-dimethylcyclohexylamine-hyptolide **(3)** and

hydroxamic acid were constructed using Avogadro software. Visualization of the ligand-protein complex was carried out using Discovery Studio Visualizer [16,17].

Results and discussion

Synthesis of *N,N*-dimetilsiklohexylamine-hyptolide (**13**)

The Diels-Alder reaction between Hyptolide **(1)** and aminosiloxy dienes **(2)** produced the cyclic compound *N,N*-dimethylcyclohexylamine-hyptolide **(3)**, adapted from the method of Kozmin *et al.* [12] with slight modifications. The reaction was carried out at 20 °C for 32 h, yielding a pale yellow-white solid with a 67% yield. The cycloaddition of Hyptolide **(1)** was performed to obtain Hyptolide derivatives with higher polarity, which is expected to enhance their cytotoxic effects *in vivo* [18]. Cycloaddition of aminosiloxy dienes **(2)** with the dienophiles methyl acrylate and dimethyl maleate at 20 °C using ether as the solvent afforded the cyclic compounds 4-carbomethoxy-3-dimethylamino-1-tert-butyldimethylsiloxy-1-cyclohexene and diethyl-4-tert-butyldimethylsilyloxy-4-cyclohexene-1,2-dicarboxylate, with yields of 98% [9] and 92% [19], respectively. After 32 h, the mixture of Hyptolide **(1)** and aminosiloxy dienes **(2)** was separated by preparative thin layer chromatography (prep-TLC) to isolate the synthesized product and any unreacted aminosiloxy dienes **(2)**. The residue was dissolved in solvent and filtered, then the filtrate was evaporated at room temperature. The crude product was further purified by recrystallization using diethyl ether to obtain a highly pure synthesized compound [19]. The purity of the synthesized *N,N*-dimethylcyclohexylamine-hyptolide **(3)** was analyzed by thin layer chromatography (TLC) using several eluents, as shown in **Table 2**. The presence of a single retention factor (Rf) value confirmed the purity of the synthesized compound.

Table 2 Thin-layer chromatography (TLC) analysis using a single eluent was performed to assess the purity of the synthesized *N,N*-dimethylcyclohexylamine-hyptolide **(3)**.

Mobile Phase	Retention factor (R_f)
Dichloromethane	0.09
Chloroform: Diethyl ether (10:1)	0.76
Dichlorometane: Ethyl Acetate (3:4)	0.84

The thin-layer chromatography (TLC) data presented in **Table 2** show that the R*f* values increase with the polarity of the eluent. The Rf values of the synthesized *N,N*-dimethylcyclohexylamine-hyptolide **(3)** and Hyptolide **(1)** were 0.76 and 0.62, respectively. This indicates that the Diels-Alder adduct, *N,N*-dimethylcyclohexylamine-hyptolide **(3)**, which contains a tertiary amine group, is more polar than Hyptolide **(1)**. Purity analysis was further assessed by melting point analysis. *N,N*-dimethylcyclohexylamine-hyptolide **(3)** exhibited a melting point of 83 - 84 °C, whereas Hyptolide **(1)** melted at 86.9 - 87.7 °C [19]. A melting point range of less than 2 °C for the synthesized compound suggests high purity [20]. The reaction scheme between Hyptolide **(1)** and aminosiloxy dienes **(2)** via the Diels Alder reaction is illustrated in **Figure 1**. Aminosiloxy dienes **(2)** possess a conjugated π-bond arranged in the *s-cis* conformation, which is optimal for participation in Diels-Alder cycloaddition reactions. The *s-cis* conformation enables effective orbital overlap between the diene and the dienophile, thereby enhancing reactivity. Additionally, the electron-donating nature of the amino group further increases the nucleophilicity of the diene [19,21]. Promoting rapid and efficient cycloaddition with suitable electron-deficient dienophiles such as Hyptolide **(1)**. Hyptolide **(1)** acts as the dienophile through its π-bond, with the cyclic lactone serving as an electron-withdrawing group [22-24]. The presence of an electron-donating group on the diene and an electron-withdrawing group on the dienophile accelerates the cycloaddition reaction rate [10,20,23].

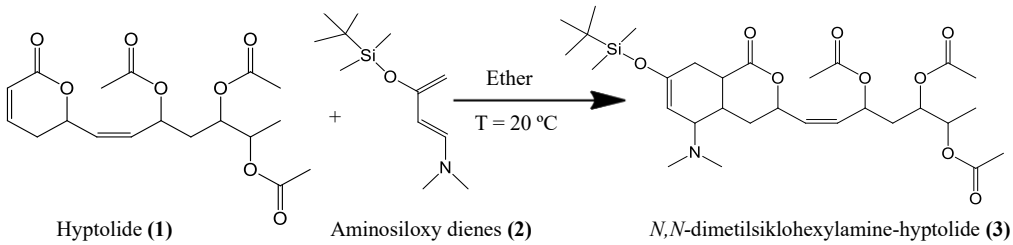

Figure 1 Reaction scheme for the synthesis of *N,N*-dimethylcyclohexylamine-hyptolide **(3)**.

Identification of functional group using FTIR

The IR spectrum of the synthesized *N,N*-dimethylcyclohexylamine-hyptolide **(3)**, shown in **Figure 2**, is consistent with previous studies [18]. Identification of the synthesized compound by IR spectroscopy revealed an absorption band at 1,357 cm^{-1}, indicating the presence of a tertiary amine (C-N) bonded to the cyclohexene ring [25]. The C-H stretching vibration of the cyclohexene was observed at 2,924 cm^{-1}. Stretching vibrations of C=C and tertiary amine (C-N) in the cyclohexene ring appeared at 1,560 and 1,357 cm^{-1}, respectively. An absorption at 1,225 cm^{-1} corresponds to the C-O lactone vibration, which was also observed in the IR analysis of Hyptolide **(1)** in previous research by Cahyono *et al.* [8]. The presence of the silyl group is indicated by absorption at 1,112 cm^{-1} [25]. The differences between the IR spectra of the synthesized *N,N*-dimethylcyclohexylamine-hyptolide **(3)** and Hyptolide **(1)** are summarized in **Table 3**.

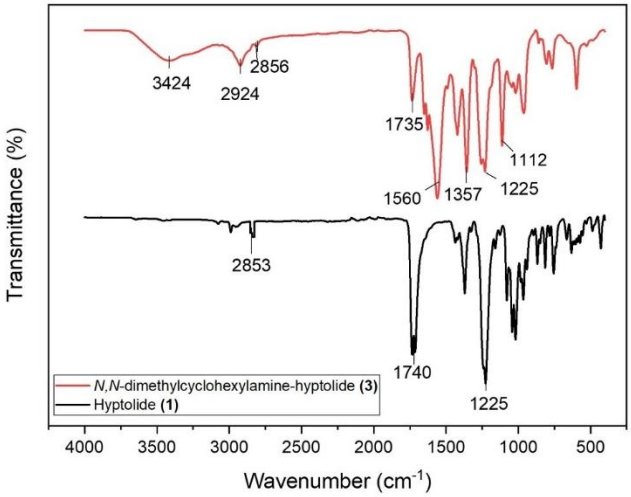

Figure 2 IR spectra of hyptolide **(1)** and the synthesized *N,N*-dimethylcyclohexylamine-hyptolide **(3)**.

Table 3 The fuctional groups data from the IR analysis of the synthesized compound *N,N*-dimethylcyclohexylamine-hyptolid*e* **(3)**.

No	Wavenumber (cm^{-1})		Functional group
	Hyptolide (1)	*N, N*-dimethylcyclohexylamine-hyptolide (3)	
1.	-	2,924	Stretching vibration of cyclohexene (C-H)
2.	2,853	2,856	Stretching vibration C-H sp3 from -CH_2
3.	1,740	-	Stretching vibration of conjugated carbonyl (C=O)
4.	-	1,560	Stretching vibration of cyclohexene (C=C)

No	Wavenumber (cm^{-1})		Functional group
	Hyptolide (1)	*N, N*-dimethylcyclohexylamine-hyptolide (3)	
5.	-	1,357	Stretching vibration of tertiery amine (C-N) from cyclohexene
6.	1,225	1,225	Stretching vibration of lactone C-O
7.	-	1,112	Stretching vibration of Si-O-C

Structure identification using ^{1}H-NMR and ^{13}C-NMR

The identification of the synthesized *N,N*-dimethylcyclohexylamine-hyptolide **(3)** compound using ^{1}H-NMR spectroscopy (in $CDCl_3$ solvent) showed results consistent with previous research conducted by Cahyono *et al.* [18]. The ^{1}H-NMR spectrum is presented in **Table 4** and **Figure 3**. The specific spectrum indicates the formation of *N,N*-dimethylcyclohexylamine-hyptolide **(3)** marked by chemical shifts (δ) at 0.23 ppm (6H), corresponding to the methyl protons on carbons C-35 and C-36 attached to silicon atoms. The second signal at δ 0.63 ppm (9H) corresponds to the methyl protons on carbons C-38, C-39, and C-30, which are bonded to carbons linked to silicon atoms. The third singlet signal at δ 2.06 ppm (6H) represents the methyl protons on C-7 and C-8 directly attached to the tertiary amine, while the fourth singlet at δ 1.96 ppm (9H) corresponds to the methyl protons of the ester groups on C-24, C-28, and C-32.

Table 4 Chemical shift data from the ^{1}H-NMR analysis of the synthesized compound *N,N*-dimethylcyclohexylamine-hyptolide **(3)**.

Carbon atom number	δ ^{1}H (ppm), multiplicity, integration
	***N,N*-dimetilsiklohexylamine-hyptolide (3)**
35, 36	0.23 (s; 6H)
38, 39, 40	0.63 (s; 9H)
7, 8	2.06 (s; 6H)
24, 28, 32	1.96 (s; 9H)
21	1.35 (d; *J* = 2.98 Hz; 3H)
15, 16	5.64 (dd; *J* = 1.0 Hz; IH)
2	5.73 (d; *J* = 1.0 Hz; 1H)
3	3.27 (t; 1H)
10	2.17 (m; *J* = 2.92 Hz dan 3.11Hz; 2H)
5	2.44 - 2.50 (m, 1H)
11	5.07 - 5.11 (m, 1H)
6	3.06 - 3.10 (m; *J* = 1.0 Hz dan 1.01 Hz; 2H)

The spectrum also clearly shows 3 doublet signals at δ 1.35 ppm (J = 2.98 Hz; 3H), corresponding to methyl protons attached to carbon C-21. A double doublet signal appears at δ 5.64 ppm (J = 1.0 Hz; 1H), assigned to the proton bound to carbons C-15 and C-16 (CH=CH), while a doublet signal at δ 5.73 ppm (J = 1.0 Hz; 1H) corresponds to the proton attached to carbon C-2 of the ethylene group (CH) in the cyclohexene structure. A triplet signal at δ 3.27 ppm (1H) is attributed to the methine proton (N-CH) on carbon C-3 in the cyclohexene ring bonded to the tertiary amine. Protons on the δ-lactone ring produce multiplet signals at δ 2.16 - 2.17 ppm (J = 2.92 and 3.11 Hz), corresponding to methylene protons (CH_2) on carbons C-10 and C-18. The multiplet at δ 2.44 - 2.50 ppm represents methine protons (CH) on carbons C-4 and C-5, and the multiplet

at δ 5.07 - 5.11 ppm (1H) corresponds to methine protons on carbons C-11, C-17, C-19, and C-20 attached to oxygen atoms in the δ-lactone ring. Additionally, multiplet signals appear at δ 3.06 - 3.10 ppm (J = 1.0 and 1.01 Hz), corresponding to methylene protons (C-6) in the cyclohexene unit, as shown in **Figure 1**. Cahyono *et al.* [9] reported that the ^{1}H-NMR spectrum of the Hyptolide derivative epoxyhyptolide does not display singlet signals at δ 0.23, 0.63, and 2.06 ppm, which are characteristic methyl (CH_3) signals derived from the 1-amino-3-siloxy-1,3-butadiene moiety involved in the Diels-Alder formation of the cyclohexene ring [18].

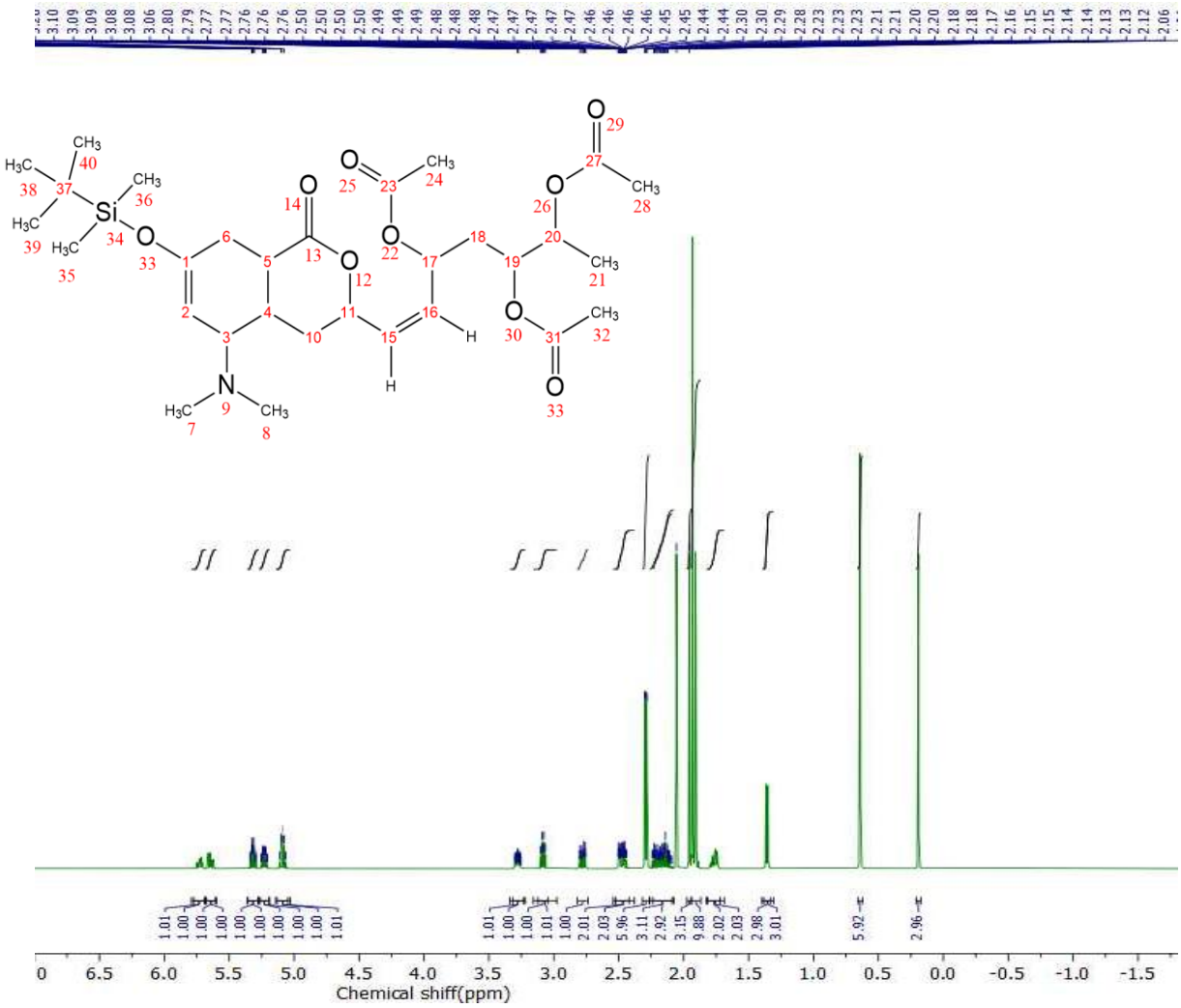

Figure 3 ^{1}H-NMR spectrum of the synthesized compound *N,N*-dimethylcyclohexylamine-hyptolide **(3)**.

The structure of the synthesized *N,N*-dimethylcyclohexylamine-hyptolide **(3)** was further confirmed by the ^{13}C-NMR spectrum shown in **Figure 4**. The spectrum shows a carbon signal at δ 146.55 ppm, corresponding to the quaternary carbon in the cyclohexene unit bonded to Si-O. Meanwhile, a signal at δ 106.54 ppm indicates the methine carbon (CH) of the cyclohexene ring. The methine carbon (CH) directly attached to the amine group appears at δ 60.21 ppm, while 2 methyl carbon (CH_3) signals bound to the amine group are observed at δ 41.14 and 42.33 ppm. Signals at δ 131.02 and 132.66 ppm correspond to the 2 methine carbons (CH=CH) of the α,β-unsaturated hyptolide unit. The quaternary carbon of the δ-lactone unit gives a signal at δ 173.49 ppm. Additionally, 3 quaternary carbons of the ester unit are observed at δ 170.32, 170.40, and 170.57 ppm. Specific signals are also indicated by the presence of 3 methyl carbon (CH_3) signals attached to the C-Si-O group, appearing successively at δ 20.03, 21.28, and 21.43 ppm.

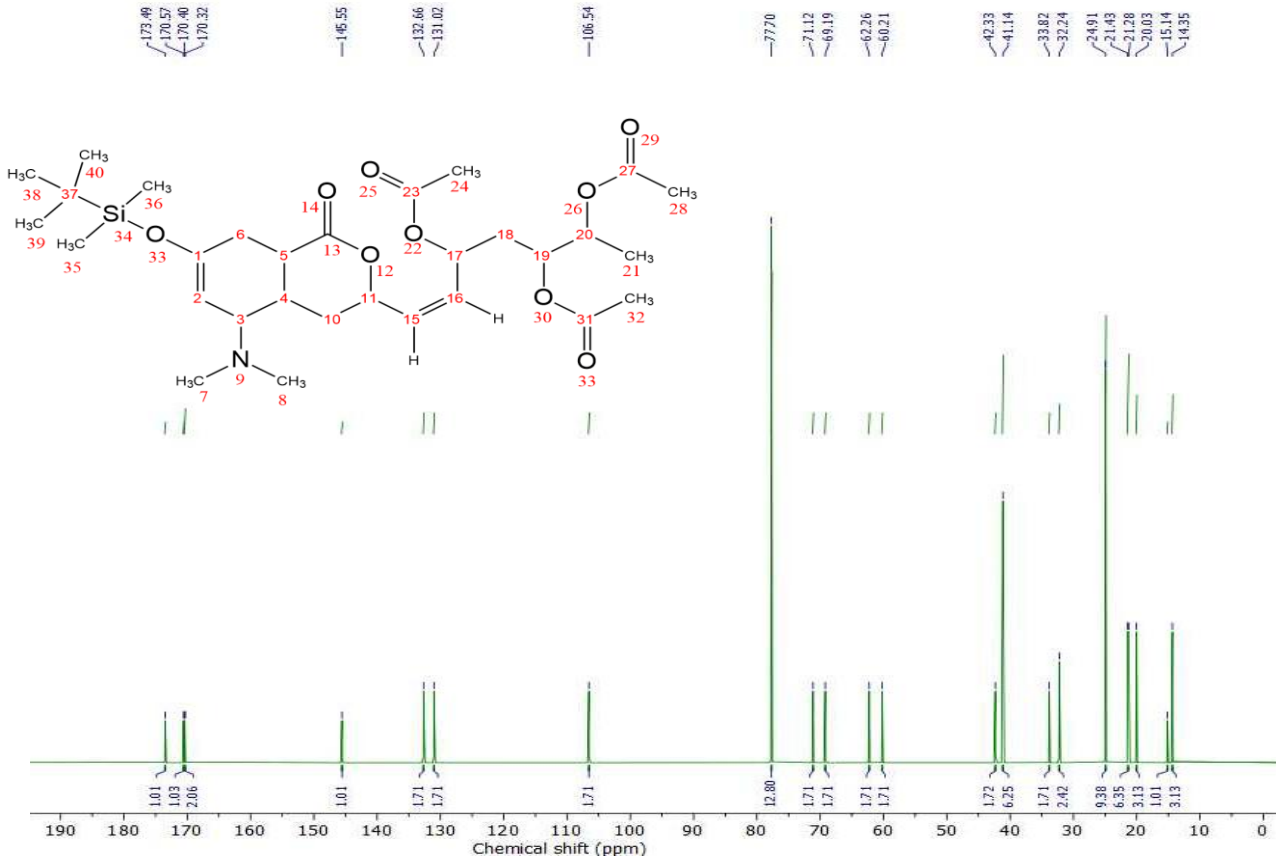

Figure 4 ^{13}C-NMR spectrum of the synthesized compound *N,N*-dimethylcyclohexylamine-hyptolide **(3)**.

Structure identification using TLC-MS

The identification of the newly formed cyclic structure within the lactone ring was further supported by thin-layer Chromatography-Mass Spectrometry (TLC-MS) analysis. The TLC-MS spectrum shown in **Figure 5** displays several peaks corresponding to the molecular weight of the synthesized compound, *N,N*-dimethylcyclohexylamine-hyptolide **(3)**. These analytical data, as summarized in **Table 5**, were compared with the theoretical molecular weight. The molecular ion peak $[M + H]^+$ of the synthesized *N,N*-dimethylcyclohexylamine-hyptolide **(3)** was observed at m/z 596.2, while the $[M + Na]^+$ ion peak was detected at m/z 618.79. These findings demonstrate strong agreement between the experimental results and the calculated molecular weights [26].

Table 5 Molecular ion data of Synthesized *N,N*-dimethylcyclohexylamine-hyptolide **(3)**.

Ion	Analytical results	Calculated results
$[M + H]^+$	596.20 (^{28}Si, ^{29}Si)	596.32 (^{28}Si, ^{29}Si)
$[M + Na]^+$	622.9 (^{28}Si, ^{29}Si)	618.79 (^{28}Si, ^{29}Si)

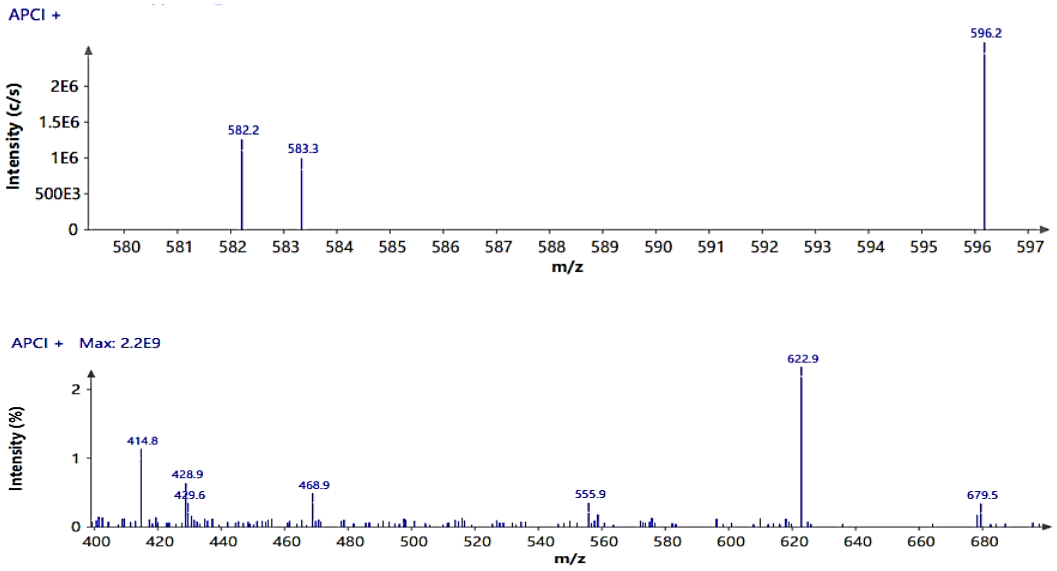

Figure 5 Positive ion APCI TLC-MS spectrum of *N,N*-dimethylcyclohexylamine-hyptolide **(3)**.

Cytotoxicity assay of the synthesized compound against breast cancer stem cells (BCSCs)

The cytotoxicity assay of the synthesized compound *N,N*-dimethylcyclohexylamine-hyptolide **(3)** was evaluated using MTT assay that demonstrated a reduction in the viability of breast cancer stem cells (BCSCs), as illustrated in **Figure 6**. BCSCs were identified based on the $CD44^+/CD24^-$ cell population, characterized by $CD44^+$ and $CD24^-$ surface expression. High levels of CD44 are correlated with tumor proggression, whereas low levels of CD24 are characteristic of undifferentiated cell populations [27,28]. The viability results of BCSCs after 24 h of incubation showed a dose-dependent decrease corresponding to increasing concentrations of *N,N*-dimethylcyclohexylamine-hyptolide **(3)**, indicating that the compound's capability to inhibit BCSC growth. The IC_{50} value of *N,N*-dimethylcyclohexylamine-hyptolide **(3)** was determined as 47.42 µg/mL, classifying the compound as moderately active. Meanwhile, the IC50 of doxorubicin against breast cancer stem cells (BCSCs) is often reported to be around 1 - 10 µM or higher [27]. This value indicates greater potency against BCSCs compared to Hyptolide **(1)** which was reported previously to have an IC_{50} of 54 µg/mL by Suzery *et al.* [14]. These findings suggest that *N,N*-dimethylcyclohexylamine-hyptolide **(3)** possesses anticancer potential comparable to Hyptolide **(1)**, with a tendency toward enhanced activity.

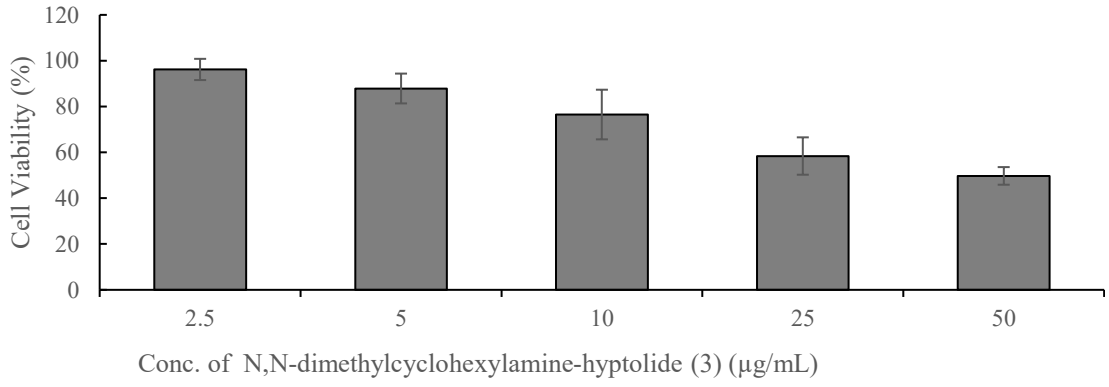

Figure 6 Viability of BCSCs following treatment with *N,N*-dimethylcyclohexylamine-hyptolide **(3)** after 24 h of incubation.

The similarity in IC_{50} values between Hyptolide **(1)** and *N,N*-dimethylcyclohexylamine-hyptolide **(3)** was further investigated by analyzing the cell cycle using 2 treatment concentrations - 55 and 110 µg/mL - via flow cytometry to explore their anti-proliferative activity. Fluorescent dyes such as propidium iodide (PI) were used for observation. Propidium iodide, a fluorescent chelating agent, binds to the DNA of dead cells and emits fluorescence at a wavelength of 526 nm [27,28,30]. The analysis results are presented in a histogram illustrating the distribution of cells across various phases of the cell cycle, as shown in **Figure 7**. The percentage distribution of each phase was analyzed under different confcentration treatments of *N,N*-dimethylcyclohexylamine-hyptolide **(3)** for 24 h on BCSCs and compared with doxorubicin as a positive control [29]. The columns represent the mean ± 5 SD from independent trials with 3 replicates and the statistical differences were analyzed using 1-way ANOVA: $*p < 0.05$. In BCSCs with doxorubicin, 0.4 ± 0.1% were in Sub G1 phase, 56.93 ± 1.7% in G0/G1 phase, 20.33 ± 0.98% in S phase and 22.33 ± 1.71% in G2/M phase [31].

The effect of *N,N*-dimethylcyclohexylamine-hyptolide **(3)** on 1/2 IC_{50} (55 µg/mL) induced the accumulation of BCSCs up to 22 ± 1.25% ($p < 0.05$) primarily in the DNA synthesis phase (S phase) and 19.7 ± 1.0% ($p < 0.05$) in the growth-to-division phase. Interestingly, in the IC_{50} dose (110µg/mL) the *N,N-dimethylcyclohexylamine-hyptolide* **(3)** induced S phase cell cycle arrest up to 26.87 ± 2.4% and G2/M phase up to 36.1 ± 3.4%. The increase in the G2/M phase population suggests cell cycle arrest at this stage. Inhibition or failure of cell division activates signaling pathways that lead to apoptosis or programmed cell death of cancer cell [32]. Suzery *et al.* [7] previously reported that Hyptolide **(1)** is capable of inducing cell cycle arrest at the G2/M phase in breast cancer stem cells. The introduction of a tertiary amine group in the synthesized *N,N*-dimethylcyclohexylamine-hyptolide **(3)** increases the polarity of the compound compared to Hyptolide **(1)**, thereby enhancing its ability to more effectively disrupt the BCSC cell cycle. The interaction between *N,N*-dimethylcyclohexylamine-hyptolide **(3)** and cell-regulating proteins in BCSCs, particularly HDAC, will be further evaluated through *in silico* analysis.

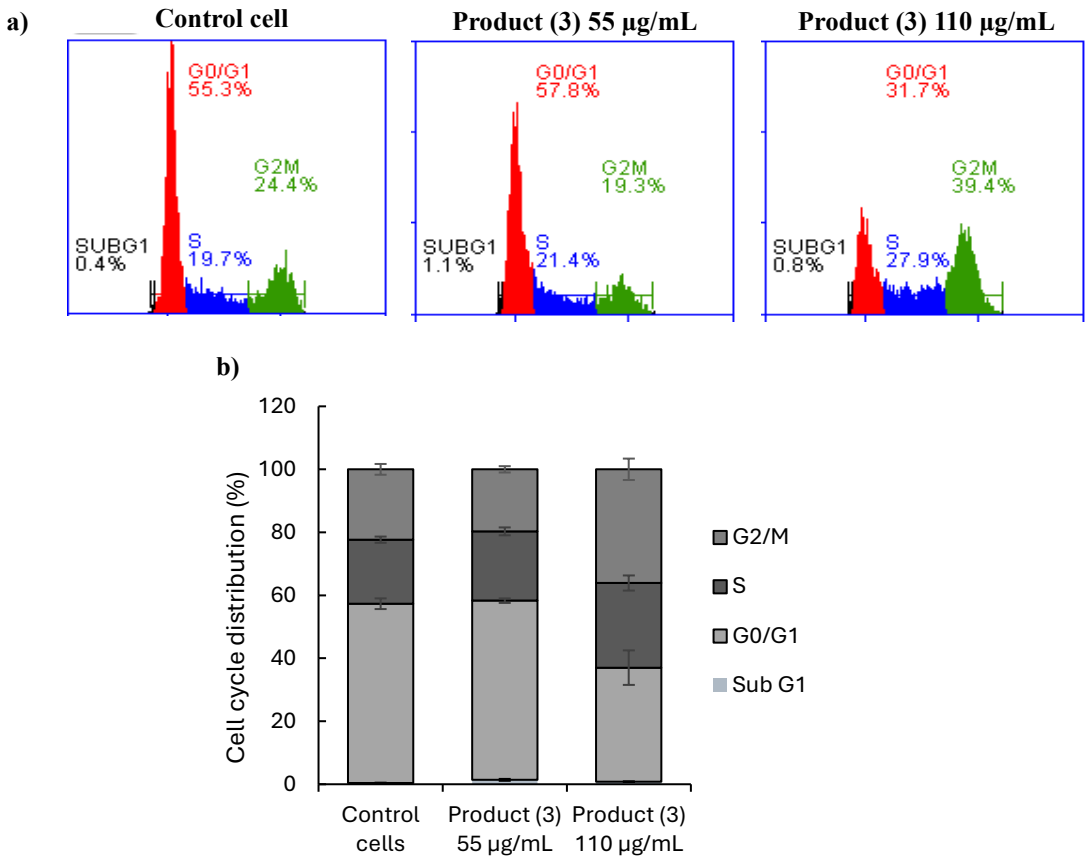

Figure 7 Cell cycle distribution profile following treatment with *N,N*-dimethylcyclohexylamine-hyptolide **(3)**. Cell cycle histogram (a), Analysis of cell population in each phase (b).

Simulations to examine the molecular docking

An *in silico* study was also conducted to support the *in vitro* findings and to better understand the inhibitory activity of *N,N*-dimethylcyclohexylamine-hyptolide **(3)** compared with the parent compound, Hyptolide **(1)** (**Figure 8**), as summarized in **Table 6**. The binding energy (ΔE), inhibitory constant (*Ki*) and binding-free energy (ΔG) of HDAC…*N,N*-dimethylcyclohexylamine-hyptolide during 0 - 50 ns molecular dynamics simulation were found to be ΔE = –27.08 kcal/mol, *Ki* = 14.41 and ΔG = 74.7 kcal/mol. A negative ΔE value (< 0) indicates that the formation of the HDAC…*N,N*-dimethylcyclohexylamine-hyptolide complex is exothermic and thermodynamically stable [33]. However, the positive ΔG value (> 0) suggests that the complex formation is non-spontaneous, implying that the interaction between the ligand and receptor does not occur naturally and requires external energy input [34]. Positive binding energy values also indicate weaker interaction between the receptor and ligand [35].

Interestingly, these results suggest that the ligand-receptor interaction is non-covalent bound. This interaction may shift slightly due to induce fit, hydrogen bonding changes, hydrophobic contacts and dynamic alterations in ligand binding, allowing for irreversible inhibition. The ligand, *N,N*-dimethylcyclohexylamine-hyptolide **(3)** momentarily block the active site in HDAC receptor, but then dissociates and behaving as a low-affinity reversible inhibitor. In this case, the non-covalently binding of *N,N*-dimethylcyclohexylamine-hyptolide **(3)** to the active site residue of the HDAC receptor results in the receptor becoming permanently inactive [36]. However, steric clashes between the protein and ligand possible due to atomic overlap, can raise the energy and produce unstable interaction within the complex [37,38].

Table 6 *In silico* HDAC inhibitory activity of HDAC…*N,N*-dimethylcyclohexylamine-hyptolide and HDAC…hyptolide.

Complexes	ΔE (kcal/mol)	ΔG (kcal/mol)	K_i (μM)	Binding site	Hydrogen bond (Å)
HDAC…*N,N*-dimethylcyclohexylamine-hyptolide	−27.08	74.7	14.41	*HIS_{670}-HE2…DCE-O_{90}	2.23
				*HIS_{709}-HD1…DCE-O_{90}	3.01
				*PHE_{738}-NH…DCE-O_{51}	2.45
				**ASP_{801}-OD2…DCE-N	5.23
				#PRO_{801}…DCE-C_{12}	4.15
HDAC…Hyptolide	−32.79	106.8	2.99	*HIS_{669}-HE2…Hyp-O_{39}	2.26
				*HIS_{670}-HE2…Hyp-O_{39}	2.14
				*HIS_{669}-HD2…Hyp-O39	2.89
				*GLY_{841}-HA1…Hyp-O_{18}	2.84
				*GLY_{841}-HA2…Hyp-O_{18}	2.05
				*PHE_{679} …Hyp-C_{10}	2.24
				*PHE_{709} …Hyp-C_2	4.65

* = Hydrogen bond; # = hydrophobic interaction; ** = Electrostatic interaction.

Several factors contribute to the non-spontaneous nature of the interaction, including the relatively high binding energy (ΔE), which indicates that the binding force required to form a stable complex is insufficient. The interaction between Hyptolide **(1)** and *N,N*-dimethylcyclohexylamine-hyptolide **(3)**, both of which have relatively bulky structures, results in low complex formation affinity [30,34]. Conversely, the lower the binding energy generated between a receptor and ligand complex, the higher the binding affinity or the likelihood of interaction between the receptor and ligand [39]. The ligand interaction sites were identified via 3 hydrogen bonds with the amino acid residues HIS_{670} (2.21 Å), HIS_{709} (3.01 Å), PHE_{738} (2.45 Å) along with hydropobic interaction involving residues of ASP_{801} (5.23 Å), and PRO_{801} (4.15 Å). The HDAC protein contains a Zn^{2+} ion chelation site that serves as its catalytic center, which binds to the active site of the ligand *N,N*-dimethylcyclohexylamine-hyptolide **(3)**.

This chelation blocks substrate access (acetyl-lysine) to the active site, thereby inhibiting the deacetylation of histone and non-histone proteins [40]. The interaction with these amino acid residues disrupts the catalytic activity of Zn^{2+}, subsequently hindering histone deacetylation and leading to chromatin relaxation, which facilitates the DNA transcription process [40-42]. The calculated binding energy was subsequently used to determine the inhibition constant (K_i), representing the concentration of the ligand *N,N*-dimethylcyclohexylamine-hyptolide **(3)** required to occupy 50% of the active sites on the HDAC receptor. A lower *Ki* value indicates a higher binding affinity between the ligand and receptor [43,44]. The inhibition constant obtained from molecular docking simulations (Ki = 14.41 μM) is relatively high ($Ki > 0$), suggesting that the ligand-receptor complex of *N,N*-dimethylcyclohexylamine-hyptolide **(3)** exhibits relatively weak inhibitory activity. While the binding energy and inhibitory constant of Hyptolide **(1)** indicated enhanced HDAC inhibitory activity (ΔE = −32.79 kcal/mol, K_i = 2.99 μM), its positive free binding energy suggests that complex formation with HDAC is also non-spontaneous. Furthermore, the major binding interaction between Hyptolide **(1)** and HDAC occur through hydrogen bonds. The lower the *Ki*, the lower the ligand concentration needed to inhibit enzyme or receptor activity. The information derived from the molecular docking analysis can also predict the controlled drug release process. The lower the binding energy, the faster the drug is expected to be released [45]. This result suggest that both *N,N*-dimethylcyclohexylamine-hyptolide **(3)** and Hyptolide **(1)** acts as an HDAC inhibitor, regulating the HDAC activity.

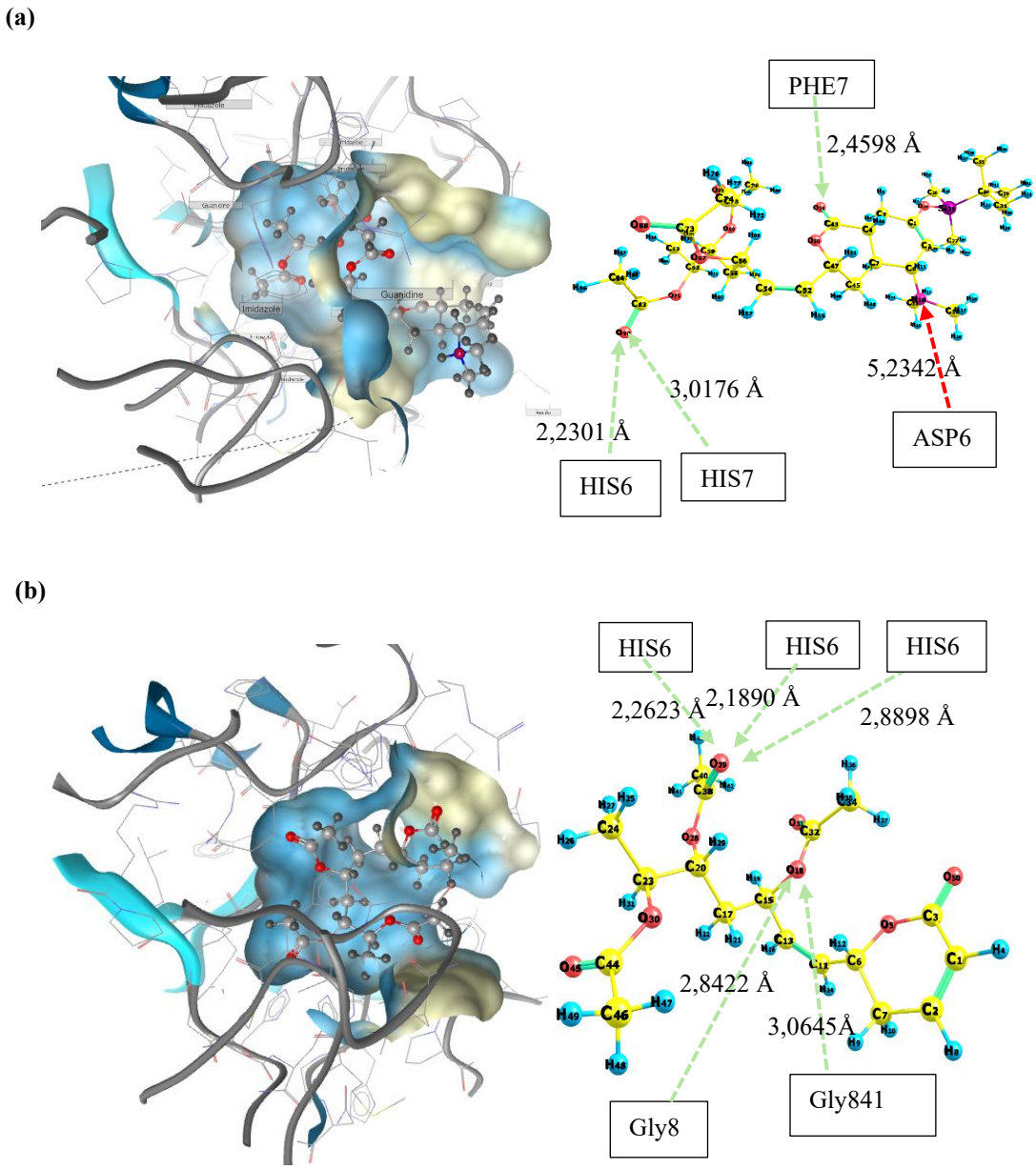

Figure 8 Interaction complexes. HDAC…*N,N*-dimethylcyclohexylamine-hyptolide **(a)** and HDAC…hyptolide **(b)**.

Conclusions

The synthesis of *N,N*-dimethylcyclohexylamine-hyptolide **(3)** was successfully achieved using aminosiloxy dienes **(2)**, yielding 67%. The compound exhibited cytotoxic activity against breast cancer stem cells (BCSCs) with an IC_{50} value of 47.42 µg/mL, classified as moderately active. *In vitro* analysis demonstrated that the compound induced cell cycle arrest at both the DNA synthesis phase (S phase) and the cell division phase (G2/M phase), indicating its potential to inhibit cancer cell proliferation. Further *in silico* molecular docking studies revealed that *N,N*-dimethylcyclohexylamine-*hyptolide* **(3)** interacts with key amino acid residues at the active site of HDAC via Zn^{2+} ion chelation. However, its binding affinity, as reflected by ΔG and Ki values, was lower than that of the parent compound Hyptolide **(1)**, suggesting a weaker inhibitory effect. These indicate that while *N,N*-dimethylcyclohexylamine-hyptolide **(3)** shows promising cytotoxic activity and HDAC interaction, further structural optimization is required to enhance its inhibitory potential.

Future studies might explore *in vivo* evaluations of the compound to assess its pharmacokinetics, efficacy,

and safety profiles comprehensively. Additionally, structural modifications to optimize target specificity, improve potency, and reduce potential off-target effects might be explored further to enhance therapeutic potential. These directions will be crucial for advancing the development of this compound as a promising anticancer agent.

Acknowledgements

This research was funded by Diponegoro University Research and Community Service Institute (LPPM-Diponegoro University) grant, Indonesia for The Riset Publikasi Internasional scheme, contract number 609-82/UN7.D2/PP/VIII/2023.

Declaration of Generative AI in Scientific Writing

The authors acknowledge the use of generative AI tools (e.g., Perplexity by OpenAI) in the preparation of this manuscript, specifically for language editing and grammar correction. No content generation or data interpretation was performed by AI. The authors take full responsibility for the content and conclusions of this work.

CRediT Author Statement

Meiny Suzery Conceptualization, Resources, Methodology, Data curation, Validation, Supervision and giving the final approval of the manuscript. **Lulut Tutik Margi Rahayu** Writing and editing original draft, Formal analysis, Data curation, Investigation, Visualization and Conceptualization. **Bambang Cahyono** Conceptualization, Validation, methodology, Data curation and Reviewing original draft. **Parsaoran Siahaan** Conceptualization, Supervision, Validation, Software, Methodology, and Data curation.

Reference

[1] N Dasari, GS Guntuku and SKSS Pindiprolu Targeting triple negative breast cancer stem cells using nanocarriers. *Discover Nano* 2024; **19(1)**, 41.

[2] SKSS Pindiprolu, PT Krishnamurthy, PK Chintamaneni and VVSR Karri. Nanocarrier based approaches for targeting breast cancer stem cells. *Artificial Cells, Nanomedicine, and Biotechnology* 2017; **46(5)**, 885-898

[3] RK Khangura, A Bali, AS Jaggi and N Singh. Histone acetylation and histone deacetylation in neuropathic pain: An unresolved puzzle? *European Journal of Pharmacology* 2017; **795**, 36-42.

[4] HR Gatla, N Muniraj, P Thevkar, S Yavvari, S Sukhavasi and MR Makena. Regulation of chemokines and cytokines by histone deacetylases and an update on histone decetylase inhibitors in human diseases. *International Journal of Molecular Sciences* 2019; **20**, 1-27.

[5] RI Jenie, ND Amalina, A Hermawan, M Suzery, A Putra and E Meiyanto. Caesalpinia sappan reduces the stemness of breast cancer stem cells involving the elevation of intracellular reactive oxygen species. *Research in Pharmaceutical Sciences* 2023; **18**, 708-721.

[6] JK Opara, S Sanchez, SM Thomas and S Anant. Natural products targeting cancer stem cells: A promising therapeutic approach. *Exploration of Drug Science* 2025; **3**, 1008106.

[7] M Suzery, B Cahyono and ND Amalina. Antiproliferative and apoptosis effect of hyptolide from hyptis pectinata (l.) poit on human breast cancer cells. *Journal of Applied Pharmaceutical Science* 2020; **10(2)**, 001-006.

[8] B Cahyono, M Suzery, ND Amalina and DN Bima. Synthesis and antibacterial activity of epoxide from hyptolide (*Hyptis pectinata* (L.) Poit) against gram-positive and gram-negative bacteria. *Journal of Applied Pharmaceutical Science* 2020; **10(12)**, 013-022.

[9] M Suzery, B Cahyono, ND Amalina, C Budiman, I Bayu and M Asy. Antiplasmodial activity of *Hyptis pectinat*a extract and its analog against 3D7 *Plasmodium falciparum* through caseinolytic protease proteolytic (ClpP) inhibition *The Thai Journal of Pharmaceutical Sciences* 2021; **45**, 527-531

[10] C V Barbosa, PGV Aquino, KAL Ribeiro-Júnior, FBP Moura, MS Alexandre-Moreira, AEG Sant'Ana, JRO Ferreira, MO Moraes, C Pessoa, JS Aguiar, TG Silva and JX Araújo-Júnior. Cytotoxic and antitumor activities of *Hyptis pectinata* (Sambacaitá) extract. *Pharmacologyonline* 2012; **3**, 70-74.

[11] FR Santana, L Luna-Dulcey, VU Antunes, CF

Tormena, MR Cominetti, MC Duarte and JA da Silva. Evaluation of the cytotoxicity on breast cancer cell of extracts and compounds isolated from *Hyptis Pectinat*a (L.) poit. *Natural Product Research* 2020; **34**, 102-109.

[12] SA Kozmin, MT Green and VH Rawal. On the reactivity of 1-amino-3-siloxy-1 , 3-dienes: Kinetics investigation and theoretical interpretation at providing fundamental quantitative information re- garding the diels - alder kinetics of amino siloxy dienes larly interested in determining if t. *The Journal of Organic Chemistry* 2002; **64(21)**, 8045-8047.

[13] EE Kwan and SG Huang. Structural elucidation with NMR spectroscopy: Practical strategies for organic chemists. *European Journal of Organic Chemistry* 2008; **2008(16)**, 2671-2688.

[14] M Suzery, B Cahyono and ND Amalina. Unveiling the potential of hyptis capitata and hyptis brevipes compounds in overcoming apoptosis resistance and inducing targeted cell cycle arrest in breast cancer stem cells. *Trends in Sciences* 2024; **21(12)**, 8404.

[15] D Hermansyah, D Munir, A Lelo, A Putra, ND Amalina and I Alif. The synergistic antitumor effects of curcuma longa and phyllanthus niruri extracts on promoting apoptotic pathways in breast cancer stem cells. *The Thai Journal of Pharmaceutical Sciences* 2022; **46(5)**, 541-550.

[16] M Ikawati, RI Jenie, RY Utomo, ND Amalina, GPN Ilmawati, M Kawaichi and E Meiyanto. Genistein enhances cytotoxic and antimigratory activities of doxorubicin on 4T1 breast cancer cells through cell cycle arrest and ROS generation. *Journal of Applied Pharmaceutical Science* 2020;**10(10)**, 95-104.

[17] MV Sefton, H Uludag, J Babensee, T Roberts, V Horvath and U De Boni. Microencapsulation of cells in thermoplastic copolymer (hydroxyethyl methacrylate-methyl methacrylate). *Methods in Neurosciences* 1994; **21**, 371-386.

[18] G Bora-Tatar, D Dayangaç-Erden, AS Demir, S Dalkara, K Yelekçi and H Erdem-Yurter. Molecular modifications on carboxylic acid derivatives as potent histone deacetylase inhibitors: Activity and docking studies. *Bioorganic & Medicinal Chemistry* 2009; **17(14)**, 5219-5228.

[19] SA Kozmin and VH Rawal. Preparation and Diels−Alder Reactivity of 1-Amino-3-siloxy-1,3-butadienes. *The Journal of Organic Chemistry* 1997; **62(16)**, 5252-5253.

[20] SF Pedersen and AM Myers. *Understanding the principle of organic chemistry a laboratory course.* 10th ed. Mary Finch Acquisitions, Virginia, United States, 2011.

[21] SA Kozmin, JM Janey and VH Rawal. 1-amino-3-siloxy-1,3-butadienes: Highly reactive dienes for the diels- alder reaction. *The Journal of Organic Chemistry* 1999; **64**, 3039-3052.

[22] S Harada and A Nishida. Catalytic and enantioselective diels-alder reaction of siloxydienes. *Asian Journal of Organic Chemistry* 2019; **8(6)**, 732-745.

[23] CJ Huang and EY Li. Molecular design principles towards exo-exclusive Diels-Alder reactions. *RSC Advances* 2019; **9(13)**, 7246-7250.

[24] A Oluwasanmi and C Hoskins. Potential use of the Diels-Alder reaction in biomedical and nanomedicine applications. *International Journal of Pharmaceutics* 2021; **604**, 120727.

[25] J Coates. Interpretation of infrared spectra, a practical approach. *Encyclopedia of Analytical Chemistry* 2000; **12**, 10815-10837.

[26] C Hao, N Sousou, D Eikel and J Henion. Thin-layer chromatography/mass spectrometry analysis of sample mixtures using a compact mass spectrometer. *American Laboratory* 2015; **47(4)**, 24-27.

[27] A Jaggupilli and E Elkord. Significance of CD44 and CD24 as cancer stem cell markers: An enduring ambiguity. *Journal of Immunology Research* 2012; **2012(1)**, 708036.

[28] NH Zakaria, N Saad, CA Che Abdullah and N Mohd. Esa. The antiproliferative effect of chloroform fraction of *Eleutherine bulbosa* (Mill.) Urb. on 2D- and 3D-human lung cancer cells (A549) model. *Pharmaceuticals* 2023; **16(7)**, 936.

[29] C Liu, H Xing, C Guo, Z Yang, Y Wang and Y Wang. MiR-124 reversed the doxorubicin resistance of breast cancer stem cells through STAT3/HIF-1 signaling pathways. *Cell Cycle* 2019; **18(18)**, 2215-2227.

[30] MC Bajgelman. *Principles and applications of*

flow cytometry. *In*: G Misra (Ed.). Data processing handbook for complex biological data sources. Elsevier, Amsterdam, Netherlands, 2019.

[31] LC Crowley, AP Scott, BJ Marfell, JA Boughaba, G Chojnowski and NJ Waterhouse. Measuring cell death by propidium iodide uptake and flow cytometry. *Cold Spring Harbor Protocols* 2016; **2016(7)**, 647-651.

[32] C Park, HJ Cha, H Lee, H Hwang-Bo, SY Ji, MY Kim, SH Hong, JW Jeong, MH Han, SH Choi, CY Jin, GY Kim and YH Choi. Induction of G2/M cell cycle arrest and apoptosis by genistein in human bladder cancer T24 cells through inhibition of the ROS-dependent PI3k/Akt signal transduction pathway. *Antioxidants* 2019; **8(9)**, 327.

[33] Z Kinart, M Hoelm and M Imińska. Evaluating theoretical solvent models for thermodynamic and structural descriptions of dacarbazine - cyclodextrin complexes. The theoretical and conductometric study. *Molecules* 2025; **30(11)**, 2309.

[34] X Du, Y Li, YL Xia, SM Ai, J Liang, P Sang, XL Ji and SQ Liu. Insights into protein-ligand interactions: Mechanisms, models, and methods. *International Journal of Molecular Sciences* 2016; **17(2)**, 144.

[35] D Hudiyanti, R Khairiah, P Siahaan, FAA Majid, E Fachriyah and NH Zakaria. Enhanced stability and binding efficiency of liposomal andrographolide complexes targeting human papillomavirus for cervical cancer therapy: Molecular docking and molecular dynamics simulations. *Results in Chemistry* 2025; **16**, 102342.

[36] VP Reddy. Fluorinated compounds in enzyme-catalyzed reactions. *Organofluorine Compounds in Biology and Medicine* 2015; **5**, 29-57.

[37] S Ramachandran, P Kota, F Ding and NV Dokholyan. Automated minimization of steric clashes in protein structures. *Proteins: Structure, Function, and Bioinformatics* 2011; **79(1)**, 261-270.

[38] TJ Gardella, H Jüppner and JT Potts. *Receptors for parathyroid hormone and parathyroid hormone-related protein*. *In*: JP Bilezikian, TJ Martin, TL Clemens and CJ Rosen (Eds.). Principles of bone biology. Academic Press, New York, 2019, p. 691-712.

[39] R Kim and J Skolnick. Assessment of programs for ligand binding affinity prediction. *Journal of Computational Chemistry* 2008; **29(8)**, 1316-1331.

[40] A Grassadonia, P Cioffi, F Simiele, L Iezzi, M Zilli and C Natoli. Role of hydroxamate-based histone deacetylase inhibitors (Hb-HDACIs) in the treatment of solid malignancies. *Cancers* 2013; **5(3)**, 919-942.

[41] F Leoni, A Zaliani, G Bertolini, G Porro, P Pagani, P Pozzi, G Donà, G Fossati, S Sozzani, T Azam, P Bufler, G Fantuzzi, I Goncharov, SH Kim, BJ Pomerantz, LL Reznikov, B Siegmund, CA Dinarello and P Mascagni. The antitumor histone deacetylase inhibitor suberoylanilide hydroxamic acid exhibits antiinflammatory properties via suppression of cytokines. *Proceedings of the National Academy of Sciences* 2002; **99(5)**, 2995-3000.

[42] PM Lombardi, KE Cole, DP Dowling and DW Christianson. Structure, mechanism, and inhibition of histone deacetylases and related metalloenzymes. *Current Opinion in Structural Biology* 2011; **21(6)**, 735-743.

[43] A Cortés, M Cascante, ML Cárdenas and A Cornish-Bowden. Relationships between inhibition constants, inhibitor concentrations for 50% inhibition and types of inhibition: New ways of analysing data. *Biochemical Journal* 2001; **357(1)**, 263-268.

[44] EC Lima, A Hosseini-Bandegharaei, JC Moreno-Piraján and I Anastopoulos. A critical review of the estimation of the thermodynamic parameters on adsorption equilibria. Wrong use of equilibrium constant in the Van't Hoof equation for calculation of thermodynamic parameters of adsorption. *Journal of Molecular Liquids* 2019; **273**, 425-434.

[45] DJ Maxwell, BC Hicks, S Parsons and SE Sakiyama-Elbert. Development of rationally designed affinity-based drug delivery systems. *Acta Biomaterialia* 2005; **1(1)**, 101-113.